Garde, A.A., Keulen, N., and Waight, T., 2021, Microporphyritic and microspherulitic melt grains, Hiawatha crater, Northwest Greenland: Implications for post-impact cooling rates, hydration, and the cratering environment: GSA Bulletin, https://doi.org/10.1130/B36058.1.

Supplemental Material

Table S1. EMP analyses of Hiawatha melt grains, detrital minerals and EMP standards, and compositions of reference points shown in Figure 15.

Figure S1. Felsic melt grain 21J-t03 with mordenite microspherulites and perlitic fractures. **(A–C)** SEM-BSE and optical images. Note cloudy microspherulitic bodies, curved perlitic fractures with alteration and late open fractures. **(D)** SEM-EDS composition map of indexed melt, quartz fragments, schlieric (presumably partly melted) feldspar fragments and alteration products. Felsic microspherulitic melt areas predominate, indexed as mordenite and Si-Al glass. Soft mesostasis partially removed by polishing, enhancing the microspherulitic structure. Perlitic fractures are lined with complex Fe-Mg-rich, phyllosilicate-bearing alteration zones. Elongate chloritic areas are interpreted as former vesicles (arrows). **(E–L)** Enlarged BSE image, indexed composition and element maps. Micro-spherulites and mesostasis are best distinguished in the BSE image, the Al map and the map of 5–10% Al on black background (**E, I, J**). All element maps in element weight percent.

Figure S2. Felsic melt grain 21J-z40 with microspherulitic mordenite, fragments of quartz and plagioclase as well as perlitic fractures with hydrothermal alteration. Mordenite microspherulites mixed with Al-Si glass predominate. **(A, B)** Optical and SEM-BSE images. **(C)**: SEM-EDS composition map with indexed melt, mineral fragments and alteration products. **(E–K)** Enlarged maps within white frame in **C**. Microspherulitic structure clearly visible in **E** and **J** (BSE and Ca maps). Thin but complex hydrothermal alteration zones have Al and K enrichment and Ca depletion, and Fe enrichment and Si depletion in their centers. All element maps in element weight percent.

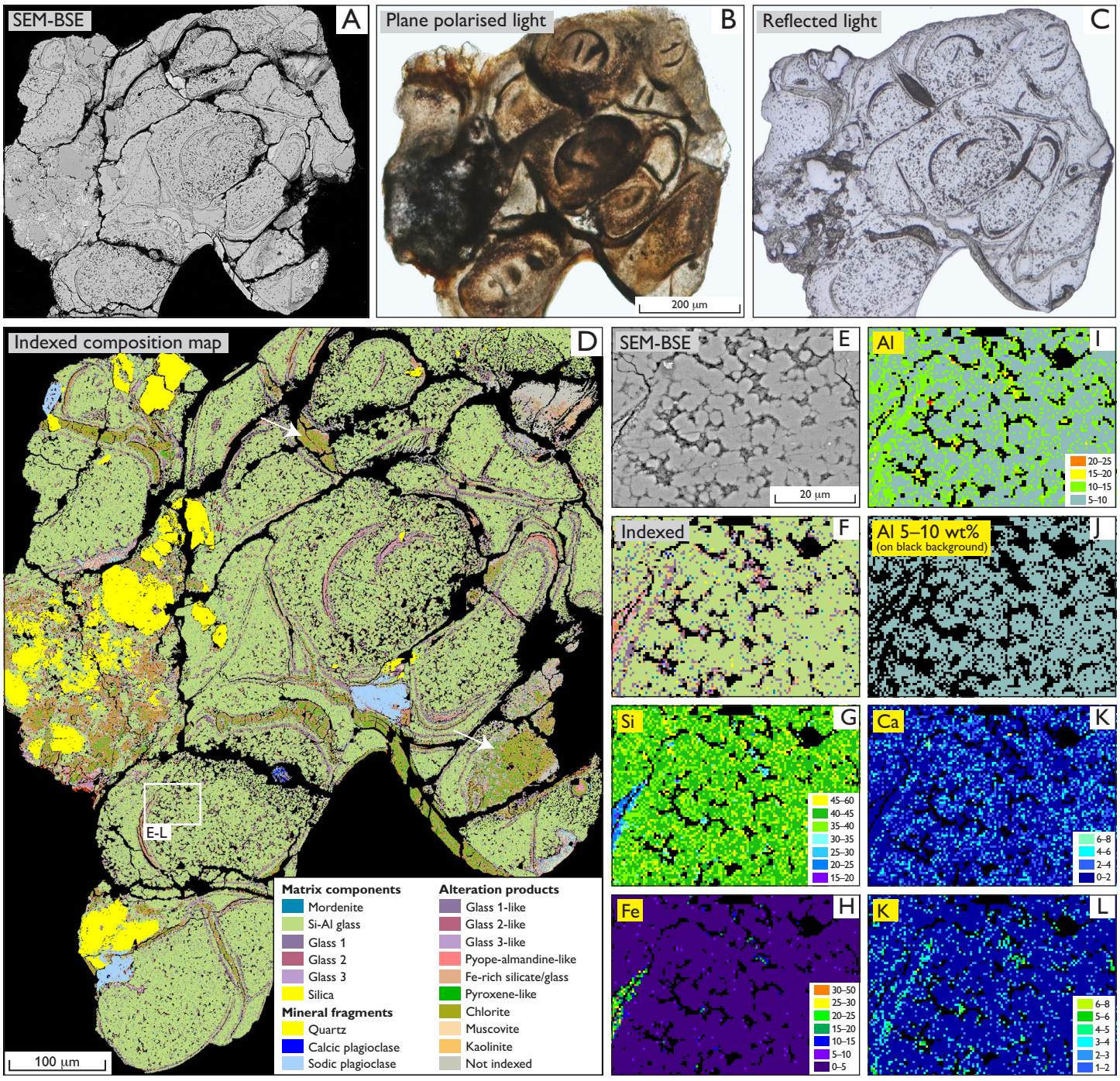
SEM-BSE
A
Plane polarised light
B
200 µm
Reflected light
C
Indexed composition map
D
E-L
100 µm
Matrix components
Mordenite
Si-Al glass
Glass 1
Glass 2
Glass 3
Silica
Mineral fragments
Quartz
Calcic plagioclase
Sodic plagioclase
Alteration products
Glass 1-like
Glass 2-like
Glass 3-like
Pyope-almandine-like
Fe-rich silicate/glass
Pyroxene-like
Chlorite
Muscovite
Kaolinite
Not indexed
SEM-BSE
E
20 µm
Indexed
F
Si
G
45–60
40–45
35–40
30–35
25–30
20–25
15–20
Fe
H
30–50
25–30
20–25
15–20
10–15
5–10
0–5
Al
I
20–25
15–20
10–15
5–10
Al 5–10 wt%
(on black background)
J
Ca
K
6–8
4–6
2–4
0–2
K
L
6–8
5–6
4–5
3–4
2–3
1–2

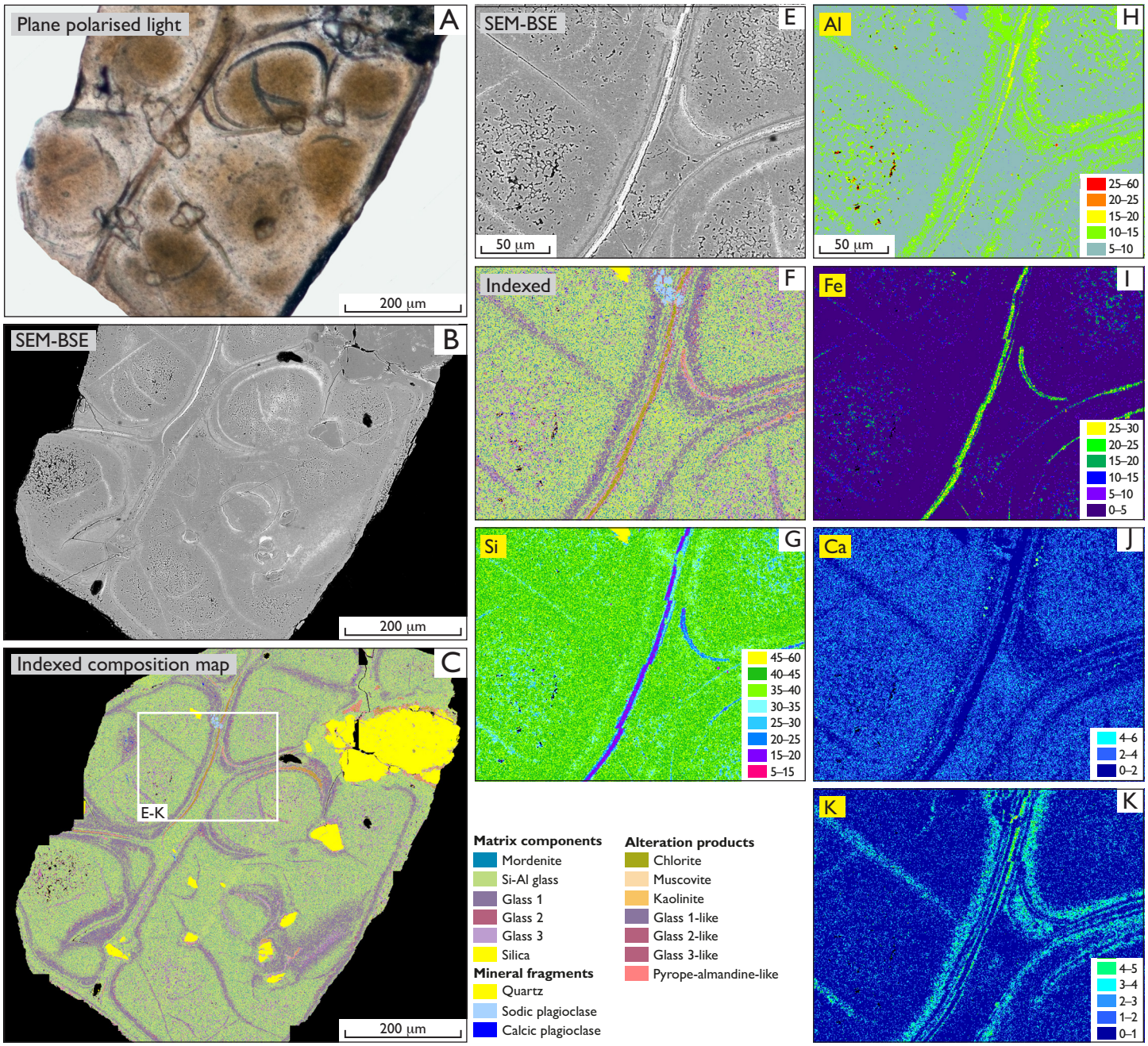
Plane polarised light
A
200 µm
SEM-BSE
B
200 µm
Indexed composition map
C
E-K
200 µm
SEM-BSE
E
50 µm
Indexed
F
Si
G
45–60
40–45
35–40
30–35
25–30
20–25
15–20
5–15
Al
H
50 µm
25–60
20–25
15–20
10–15
5–10
Fe
I
25–30
20–25
15–20
10–15
5–10
0–5
Ca
J
4–6
2–4
0–2
K
K
4–5
3–4
2–3
1–2
0–1
Matrix components
Mordenite
Si-Al glass
Glass 1
Glass 2
Glass 3
Silica
Mineral fragments
Quartz
Sodic plagioclase
Calcic plagioclase
Alteration products
Chlorite
Muscovite
Kaolinite
Glass 1-like
Glass 2-like
Glass 3-like
Pyrope-almandine-like